The Journal of Chemical Physics

Characterization of oxygen phases created during oxidation of Ru(0001)

Cite as: J. Chem. Phys. **112**, 4779 (2000); https://doi.org/10.1063/1.481034
Submitted: 21 September 1999 . Accepted: 16 December 1999 . Published Online: 28 February 2000

A. Böttcher, H. Conrad, and H. Niehus

View Online Export Citation

ARTICLES YOU MAY BE INTERESTED IN

Formation of subsurface oxygen at Ru(0001)
The Journal of Chemical Physics **110**, 3186 (1999); https://doi.org/10.1063/1.477839

Oxide-free oxygen incorporation into Ru(0001)
The Journal of Chemical Physics **120**, 3871 (2004); https://doi.org/10.1063/1.1643724

Very high atomic oxygen coverages on Ru(001)
Journal of Vacuum Science & Technology A **10**, 2565 (1992); https://doi.org/10.1116/1.578100

Challenge us.
What are your needs for periodic signal detection?
Watch
Zurich Instruments

AIP Publishing

© 2000 American Institute of Physics.

Characterization of oxygen phases created during oxidation of Ru(0001)

A. Böttcher[a] and H. Conrad
Fritz-Haber-Institut der Max-Planck-Gesellschaft, Faradyweg 4-6, 14195 Berlin, Germany

H. Niehus
Institut für Physik der Humboldt-Universität, Invalidenstr. 110, 10115 Berlin, Germany

(Received 21 September 1999; accepted 16 December 1999)

Thermal desorption spectroscopy, ultraviolet photoelectron spectroscopy, low energy electron diffraction (LEED), and the reactive scattering of a CO molecular beam have been applied to determine the relationship between the formation of the subsurface oxygen phase and the growth of oxides during oxidation of Ru(0001). Emission of RuO_x ($x<4$) molecules observed in the thermal desorption spectra during the heating of the oxygen-rich sample has been used as a simple measure for the presence of bulk oxides. When performing the oxygen exposure at a temperature lower than the onset for oxygen desorption ($T_p<850$ K) a mobile atomic oxygen species is predominantly formed in the subsurface region. The conversion of these subsurface oxygen atoms into a regular Ru_xO_y phase takes place within the temperature region of 900–1150 K. The growth of oxide films becomes the dominating reaction channel when performing the oxidation at temperatures higher than the onset for oxygen desorption. The oxide formation is strongly reduced when conducting the oxidation at temperatures higher than 1250 K. In this case only a relatively low amount of oxygen atoms adsorbed on the bare Ru surface can be achieved, neither oxides nor subsurface oxygen have been found. The presence of a RuO_2 coating layer manifests itself by LEED patterns characteristic for a particular RuO_2 single crystal face as well as by additional features in the valence ultraviolet photoelectron spectra. The oxidation of CO molecules reactively scattered at these oxygen-rich surfaces proceeds as long as mobile oxygen atoms are present in the subsurface region. The reaction is entirely quenched when the subsurface oxygen is replaced by an uniform film of RuO_2. © *2000 American Institute of Physics.* [S0021-9606(00)71010-5]

INTRODUCTION

The rapidly growing technological importance of ruthenium and its oxides as materials distinguished by their extraordinary properties was a stimulating aspect for this work. Application of ruthenium supported catalysts for an industrial-scale hydrogenolysis or Fisher–Tropsch synthesis belongs to the most spectacular developments where the unique properties of this material can be exploited in practice.[1–4] There are also numerous examples showing that doped Ru oxides might form superconducting materials, e.g., Ref. 5.

We focus here on the changes of surface properties of solid ruthenium effected by various oxidation procedures. This particular choice is motivated by two recent findings: First, it has been demonstrated that the Ru surface can be used as a kind of storage capable of accommodating large amounts of atomic oxygen.[6,7] Other transition metals exhibit this ability as well, but the exceptional property of ruthenium surfaces consists of the fact that oxygen can be completely removed by simply heating the sample up to about 1700 K without creating oxide irreversibly incorporated in the bulk. Second, it has been demonstrated that the CO oxidation reaction performed at an oxygen-rich Ru(0001) surface at elevated temperatures becomes much more efficient when the sample comprises a subsurface-oxygen phase.[8] In this case the integral reaction yield is by about two orders of magnitude higher than for samples with an adsorbed oxygen layer only. These two findings account for the enormous catalytic activity of ruthenium for the CO oxidation reaction conducted under high-pressure oxidizing conditions.[9] Two concepts have been deliberated for explanation of the subsurface-oxygen conditioned reactivity enhancement: Oxygen atoms located between the first two Ru layers induce a redistribution of the electron density also at the topmost surface layer. In consequence, the activation barrier for the reaction of CO with the topmost oxygen atoms is significantly lowered. The second concept takes into account the subsurface-oxygen phase as consisting of mobile oxygen atoms which can participate in the CO oxidation only via thermal diffusion after reaching the topmost surface layer. Recent molecular beam studies of the CO-oxidation kinetics support the latter alternative identifying the thermal diffusion of subsurface oxygen atoms as the reaction limiting step.[10] It is obvious that oxygen dissolved/incorporated in a solid modifies the structure and the electronic properties of the topmost surface layer.[11–17] For instance, the Ru(0001) surface containing a large amount of oxygen in the subsurface region provides new adsorption sites for oxygen at the topmost surface layer which allow a new oxygen phase to be created. Such kind of oxygen bond does not exist at a bare Ru surface. Moreover, this phase is found to be strongly

[a]Author to whom correspondence should be addressed; electronic mail: boettcher@fhi-berlin.mpg.de

 © 2000 American Institute of Physics

involved in the CO-oxidation reaction even when performing this reaction at room temperature, it raises the probability for CO/CO_2 conversion by one order of magnitude.[18]

The present work continues our investigations concerning the incorporation of oxygen at solid Ru(0001). Since the exposures and temperatures applied in our previous studies to create subsurface oxygen loads are close to the regime where Ru can be transformed into a variety of oxides we investigated this reaction channel in more systematic way. By tracing the emission of O_2 and RuO_x ($x<4$) in thermal desorption spectroscopy we were able to distinguish between the subsurface-oxygen phase and the regular oxides, and additionally to characterize the preparation conditions for which either one is formed as the predominant phase. The geometric and electronic modifications of the surface induced by oxide growth manifests itself by additional low energy electron diffraction (LEED) patterns and characteristic ultraviolet photoelectron spectroscopy (UPS) features, respectively. A very important means for the distinction of the two phases is provided by their reactivity with respect to the CO oxidation reaction. We found the RuO_2 layers to almost totally suppress the formation of CO_2 in that temperature region where subsurface oxygen showed maximum reactivity. Only at much higher temperatures where the surface oxides become volatile and also oxide decomposition takes place does the reaction resumes.

EXPERIMENT

The apparatus and the applied experimental techniques were described in detail elsewhere.[7,8] The ultrahigh vacuum chamber is equipped with standard facilities for preparation and characterization of metallic surfaces (LEED, quadruppole mass spectrometry, Auger, UPS). The analysis chamber is connected to a two-stage molecular beam apparatus which is employed for reactive scattering experiments, in particular for the determination of the sticking coefficient. The base pressure in the chamber connected to the molecular beam sector does not exceed the limit of 10^{-10} mbar and the mass spectrum of the residual gas is characteristic for a system pumped by a turbomolecular pump. The molecular beam is mechanically chopped with a constant frequency in the range of 150–350 Hz and the scattered beam pulses are monitored by a mass spectrometer arranged in specular direction.

The Ru(0001) single crystal was cleaned according to the procedure described by Madey, Engelhardt, and Menzel.[19] The sample is treated by a series of sputtering and oxidizing cycles followed by an annealing flash up to 1550 K. The chemical cleanliness was examined by UPS and thermal desorption spectroscopy (TDS) as well as by metastable deexcitation spectroscopy. The roughness of the surface was controlled by applying specular He scattering.[20]

Thermal desorption spectroscopy has been performed by resistive heating of the sample with a constant heating rate of 6 K/s. The sample temperature was monitored by a Ni/NiCr thermocouple spotwelded to the back side of the crystal. The UP spectra of the Ru valence region have been measured by means of a hemispherical electron energy analyzer which collects the photoelectrons emitted in normal direction with an energy resolution better than 0.4 eV.

The CO beam is formed by supersonic gas expansion from a nozzle which provides a narrow velocity distribution of the impinging molecules (diameter 20 μm, input CO pressure in the range 2–4 bar). The nozzle temperature can be varied within the range of 300–900 K. The molecular flux has been determined by comparing the CO coverage achieved by the scattering of the CO beam onto a bare Ru(0001) surface to that obtained when exposing the same surface to CO at a known partial pressure in the chamber. The steady-state CO flux can be varied within the range of $0.6-4\times10^{14}$ molecules/cm^2 s. The area fraction of the crystal accessible to the CO beam has been determined in two experiments. The specularly scattered CO beam at 700 K sample temperature has been monitored whereas the sample was shifted in a direction parallel to the surface. In this way the beam diameter of 4.5 mm has been determined. In the second experiment the CO thermal desorption (TD) spectra were taken after creating a saturated layer via either exposure to the CO molecular beam or backfilling of the chamber. Integration of the TD traces revealed a ratio of 0.85, which obviously represents the upper limit for the crystal area exposed to the CO beam. The reaction yield has been corrected by this effective reaction area.

The atomic ordering of the surface was monitored with a four grid LEED optics. Surface exposure was carried out according to the procedure applied by us for the formation of a well-defined subsurface-oxygen phase,[7] i.e., by exposing the surface to molecular oxygen at partial pressure in the range of 10^{-3} mbar at a fixed sample temperature. The oxidation procedures were performed within the wide temperature region of 300–1600 K. The resulting oxygen load was determined via TDS. A precise determination of the oxygen coverage corresponding to a monolayer, $\theta_0=1$, was achieved by correlating the LEED patterns with O_2 TD spectra. Lateral saturation of the oxygen adlayer manifests itself by very sharp intense LEED spots in a (1×1)-O pattern corresponding to a lateral oxygen density of 1.58×10^{15} cm^{-2} which is the atomic density of the substrate. The oxygen content in the subsurface is expressed here in terms of a monolayer (ML).

RESULTS AND DISCUSSION

It is known that the oxidation of a polycrystalline Ru sample results in a variety of different oxygen-rich layers whose morphology, structure, and electronic properties strongly depend on the applied oxidation procedure.[21–23] Our previous study was focused on the characterization of various oxygen states by analyzing predominantly the thermal desorption of oxygen. Here we extend this study by monitoring the possible formation of oxides over a much wider range of oxidation temperatures. We start with the oxidation procedure which leads to oxygen dissolution and to formation of a very reactive subsurface-oxygen phase.[7,8] By exposing the clean Ru(0001) surface kept at $T_p=750$ K to oxygen at a partial pressure of 5×10^{-3} mbar (5×10^5 L) an oxygen load corresponding to the equivalent of 7.6 ML was created. The corresponding O_2 TD spectrum is shown in Fig. 1 (thin line). There are three well distinguishable oxygen states: The high-temperature desorption range represents oxygen atoms

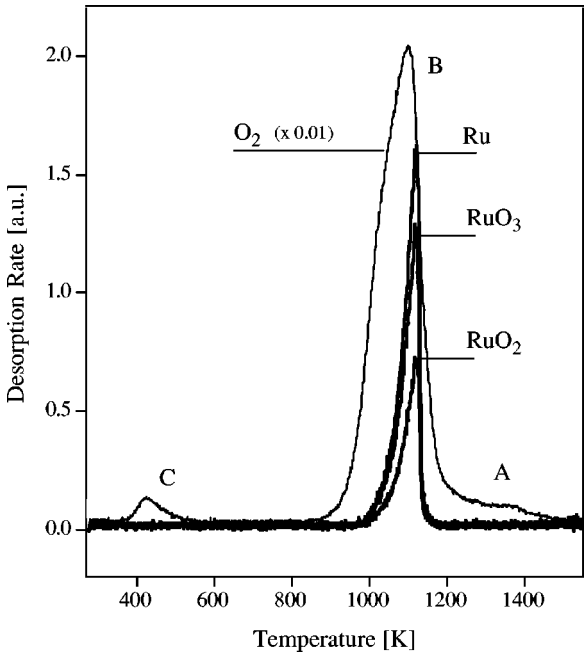

FIG. 1. Emission of Ru atoms, RuO_2 and RuO_3 molecules as monitored during the heating of a Ru(0001) surface containing 7.6 ML of oxygen (fat traces). The sample was prepared by exposing the clean Ru(0001) surface kept at 750 K to 5×10^5 L of oxygen at partial pressure of 5×10^{-3} mbar. For comparison the corresponding O_2 TD spectrum (thin trace). It reveals three different oxygen states described in the text.

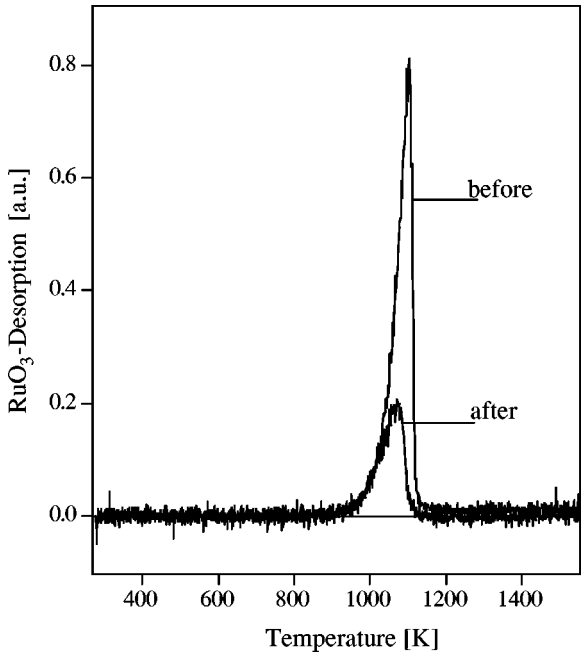

FIG. 2. Two RuO_3 TD spectra taken from an oxygen-rich Ru surface before and after exposing it to 500 L of CO at 675 K. The surface initially contained 5.3 ML of oxygen. The CO-oxidation reaction has been used as a convenient chemical tool depleting the initial oxygen content without raising the sample temperature.

chemisorbed on a clean Ru surface and arranged in the two-dimensional ordered phase, 1×1-O (state *A*).[24–27] The dominating desorption feature around 1100 K (state *B*) represents the majority of oxygen species, i.e., the subsurface oxygen atoms escaping from the surface as molecules due to their associative recombination.[7,14–17] The low-temperature desorption feature (state *C*) appears only for surfaces oxidized at elevated temperatures and additionally exposed to oxygen at 300 K. This phase consists of very weakly bound oxygen atoms which exhibit an extremely high reactivity with respect to the CO oxidation.[18]

In addition to O_2 TD Fig. 1 also shows that an emission of RuO_x ($x<4$) molecules takes place within the temperature interval of the subsurface-oxygen desorption. It overlaps with the high-temperature shoulder of the O_2 desorption. Since all the fragments exhibit a similar desorption profile they might reflect the cracking pattern of a higher-valent Ru oxide. This possibility can, however, be excluded because no signal from larger molecular species has been detected, such as RuO_4 Ru_2O_4, etc. The onset for the thermal removal of the subsurface-oxygen phase is located at $T_D=850$ K, i.e., about 100 K below the oxide emission onset. Hence, the activation energy for thermal removal of the RuO_x molecules must be considerably higher than the value of 2.3 eV found for the desorption of oxygen atoms from the subsurface region.[7,17]

The obvious question as to whether the oxides are formed already during the exposure time or dynamically in the course of the flash can be answered by utilizing the high reactivity of subsurface oxygen for CO oxidation. As shown before, even at temperatures as low as 675 K, the amount of subsurface oxygen becomes substantially depleted after CO exposure.[10] By preparing the sample twice in the same way but exposing in one experiment the sample additionally to 500 L CO at 675 K we obtained the two desorption spectra shown in Fig. 2. The strong reduction of the RuO_3 signal after the CO exposure definitely proves that no oxides are created at the preparation stage. Their formation must occur as a reaction channel competing with the diffusion-mediated oxygen desorption, i.e., within a temperature range of 850–1100 K. Moreover, the quantity of oxide formed correlates with the amount of predeposited subsurface oxygen. This is demonstrated in Fig. 3. The two RuO_3 TD spectra differ only by the initial oxygen content of the sample. Only the exposure time has been altered. Exposure temperature (800 K) and oxygen pressure (5×10^{-3}) were identical in both cases. The yield of the oxide emission follows the changes of the total oxygen content predeposited. Also, the high-temperature cutoffs for O_2 and RuO_3 desorption shifts concurrently with the increasing oxygen content. The increased number of oxygen atoms passing the surface prior to desorption gives rise to an enhanced yield of Ru_xO_y compounds in agreement with the concept of two competing reactions. Although a detailed analysis of the desorption kinetics is prohibited by the lack of knowledge about the spatial distribution of the subsurface oxygen, the shape of the desorption curves suggests a zero-order kinetics by both the common leading edge and the steep cutoff, shifted upward for the 24 ML peak. By fitting the edge to an Arrhenius function the value of 3.1 ± 0.1 eV was found as the activation energy for the removal of RuO_3. Virtually identical values have been obtained for the other emitted molecular fragments, Ru, RuO, and RuO_2. It has to be noted that the energy necessary

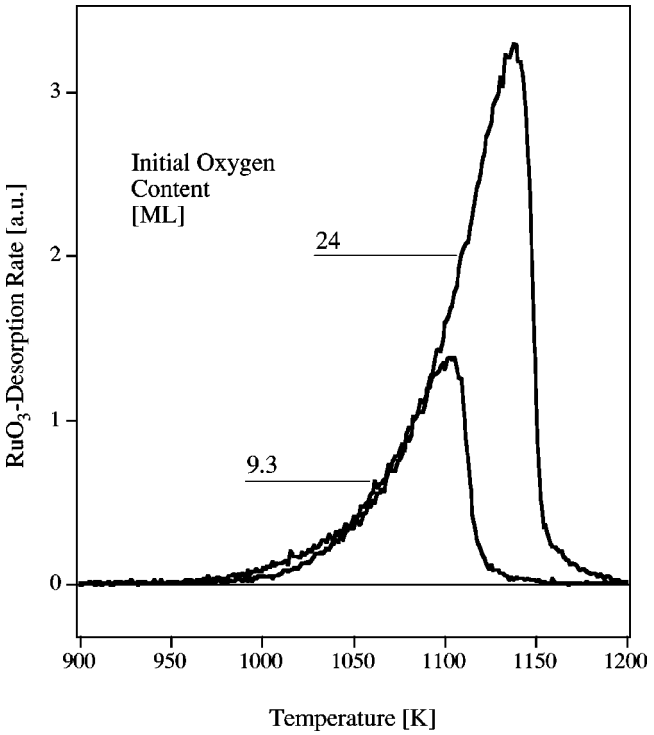

FIG. 3. Thermal desorption of RuO_3 molecules from two Ru surfaces containing 9.3 and 24 ML of oxygen. The higher oxygen content was obtained by prolongation of the exposition time. In both cases the preparation was carried out under an oxygen pressure of 5×10^{-3} mbar and at sample temperature of 800 K.

to remove a single RuO_2 molecule from a solid RuO_2 crystal requires an energy of about 4.4 eV.[28,29] Thus, the RuO_x aggregates created by the conversion of the dissolved oxygen are marked by considerably weaker bonds to their environment as is the case in the RuO_2 crystal. Similarly, the emission of Ru atoms in the temperature region of 900–1100 K signalizes a substantial destabilization of the surface in comparison with a clean Ru(0001). The heat of vaporization for the latter surface is 140 kcal/mol (melting point at 2607 K), implying that no emission of any particles can occur within the temperature range of 900–1100 K.[4] Quite similar emission of RuO_x fragments was reported for Ru(0001) exposed to NO_2.[6] This accordance indicates that the bond state of the incorporated oxygen atoms and not the unique reactivity of NO_2 is responsible for the resulting surface destabilization. The oxygen-induced destabilization of ruthenium surfaces has also been revealed by field ion microscope studies.[30] The Ru atoms as well as the oxygen species could be removed from oxygen-rich surface layers at a lower potential as compared to a clean Ru surface.

When looking at the intense RuO_x emission observed in a narrow temperature region the question arises about the chemical and geometrical state of the surface after removing the oxides. Thus we checked the reversibility of an oxidation-desorption cycle. No emission of any oxygen or oxide molecules could be observed when reheating the sample without depositing oxygen anew. The oxide emission is completed at temperatures around 1300 K and by continuing the heating the surface roughening caused by the removal of some molecular fragments becomes efficiently repaired due to annealing. This thermal smoothing of the surface was monitored by diffuse He scattering. The mean surface roughness reached that of the clean Ru surface after keeping the surface at 1550 K for only 3 s. In this way the oxidation-desorption cycle leaves a clean and almost perfect Ru surface behind.

As mentioned at the beginning, the experiments described earlier were conducted with surfaces exposed to oxygen at temperatures lower than the onset for oxygen desorption T_D, where the oxidation procedure predominantly leads to the formation of mobile oxygen atoms in the subsurface region. In order to find possible physical limits for the existence of this phase we performed the oxidation procedure at temperatures T_p higher than T_D for the same exposure conditions. Figure 4(a) shows the resulting O_2 TD spectra obtained for surfaces prepared at T_p within the range of 825–1150 K. Up to $T_p \approx 1000$ K the capability for oxygen accommodation is strongly enhanced whereby the majority of oxygen atoms populate the subsurface phase. Simultaneously, a new state develops with the desorption maximum at higher temperatures. It appears initially as a shoulder but grows in intensity until it becomes the dominating feature for T_p between 1050 and 1075 K. Concomitantly, the contribution from the subsurface-oxygen begins to decrease for $T_p > 1000$ K and is essentially zero at T_p higher than 1150 K. No oxygen desorption is observed for T_p beyond 1150 K. The new state can be tentatively attributed to the thermal decomposition of various RuO_x molecules as the major constituents of an oxide layer formed already during exposure. Accordingly, oxygen desorbs only via recombination of two oxygen atoms originating from the decomposition of some form of Ru_xO_y molecules. This process seems to be most likely because of the rather low activation energy of < 0.5 eV for the thermal decomposition, $RuO_x \rightarrow RuO_{x-1}$, calculated by Anderson and Awad[31] for single RuO_x molecules deposited on a Ru surface.

Now we turn to the complementary reaction channel, i.e., we have to answer the question, how the RuO_3 emission becomes modified when performing the oxidation at temperatures above the onset of the oxygen desorption T_D. Figure 4(b) shows the corresponding desorption profiles obtained for surfaces exposed to the identical oxygen dose of 5×10^5 L at different temperatures T_p. Two temperature regions are clearly distinguishable from the sequence of the RuO_3 spectra. For T_p lower than about 970 K, similar to the oxygen desorption [Fig. 4(a)], the oxide emission grows with increasing preparation temperature concomitant with an extension of the falling edge to higher temperature. In contrast, for T_p higher than about 970 K the opposite is the case, the RuO_3 emission strongly lessens with now the leading edge shifting to higher temperatures. For T_p above 1150 K the RuO_3 emission disappears completely.

A plausible explanation of the data presented in Fig. 4 is found by considering the very restricted stability region of the Ru oxides. If no oxide is created during the preparation the dynamic oxide formation starts during the thermal scan at about 1000 K, as shown in Figs. 1 and 2. This reaction proceeds at higher temperatures as long as sufficient oxygen is

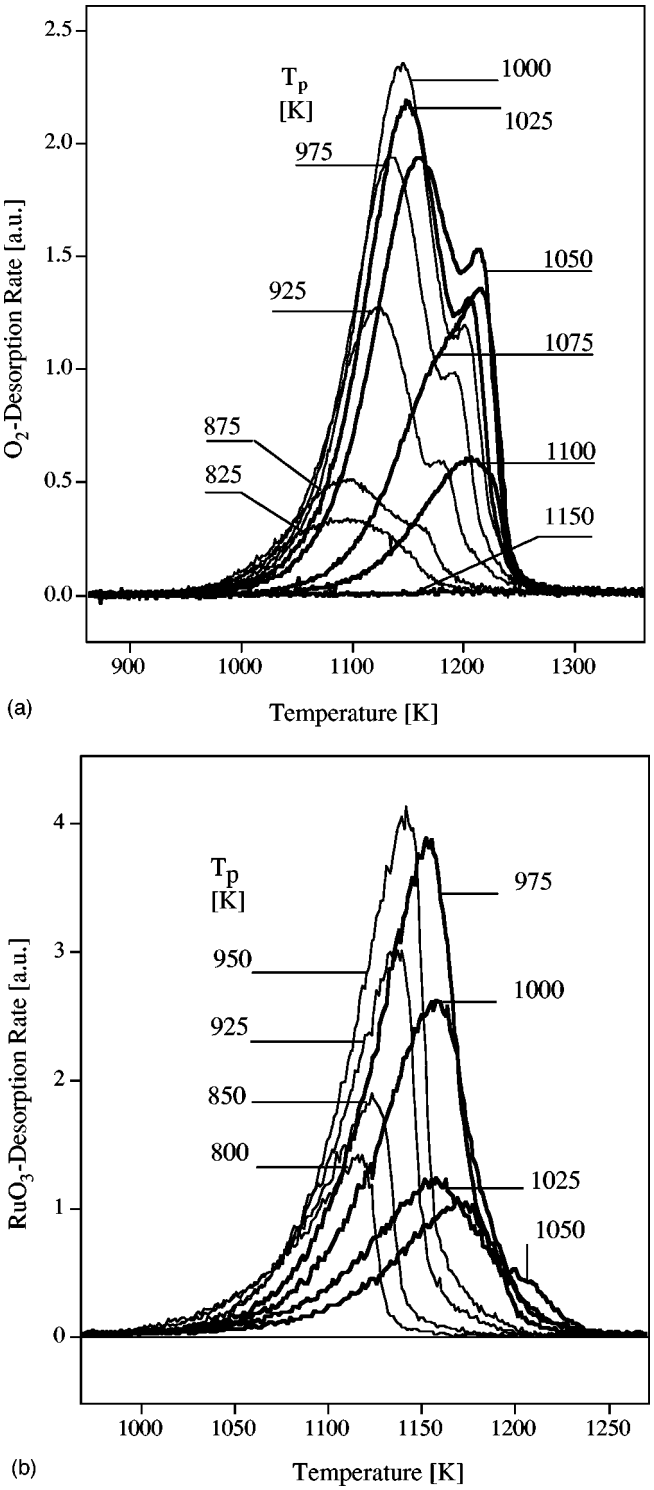

FIG. 4. (a) O_2 TD spectra obtained after exposing the surface to 5×10^5 L of oxygen at fixed sample temperatures T_p within the range of 825–1150 K. The preparation temperatures chosen here cover the region where the oxygen desorption takes place, i.e., in this region the oxides growth competes with oxygen removal. (b) RuO_3 TD spectra taken after applying the same oxidation procedure at different temperatures T_p within the region of 750–1100 K.

available in the subsurface region. Both channels are mirrored in the TD spectra shown in Figs. 4(a) and 4(b) as thin line curves. But already at preparation temperatures about 850 K a second O_2 desorption state starts to develop, it finally reaches a maximum at about 1200 K. We interpreted this emission as being due to thermal decomposition of the Ru oxides which begins to be a stable component for oxidation temperatures above 850 K. As apparent from Fig. 4(a) the oxide becomes the dominating phase with increasing oxidation temperatures, while less of the admitted oxygen is deposited in the subsurface region. From 1050 K on, almost all oxygen exists as oxide until at $T_p\approx1150$ K, no stationary oxygen phase is produced. The intermediate stage (subsurface oxygen and oxides) is also clearly reflected in the series of RuO_3 desorption spectra. As long as a part of RuO_3 is dynamically created, the leading edge stays roughly between 1000 and 1100 K, although the growing amount of the stationary oxide phase manifests itself by a shift of the decreasing flank to higher temperature thereby shifting the apparent maximum to higher temperature as well. Above $T_p\approx1000$ K, the falling edge becomes stable while the rising edge shifts to higher temperature. This must be connected with the fact that Ru oxide is the majority species formed. Moreover, the stable position of the falling edge of the RuO_3 desorption peak is strong evidence that the decrease of the RuO_3 emission is not due to a reduction of the oxide phase during preparation but reflects its thermal decomposition. As apparent from Fig. 4(a), the O_2 emission resulting from oxide dissociation passes the maximum at about 1200 K, clearly above the RuO_3 desorption maximum.

Figure 5 compares the total oxygen content with the RuO_3 emission, both as functions of the preparation temperature T_p. It must be noted that while the oxygen content is given in ML equivalents the RuO_3 emission could not be calibrated against O_2. Smaller RuO_x molecules, namely RuO and RuO_2, exhibit the same dependence on the preparation temperature T_p. The resulting amount of oxides clearly depends on the sample temperature T_p. It reflects the above discussed temperature conditioned dynamic balance between the formation, decomposition, and removal of various oxygen species appearing at the surface as intermediates. Above $T_p=1150$ K neither oxides nor subsurface oxygen could be found. There are two possible explanations: either the Ru oxides cannot be formed because of the vanishing sticking probability for the impinging oxygen molecules, or the created oxides become immediately decomposed and/or removed from the surface. The former possibility is rather unlikely since the measurements of the initial sticking coefficient performed recently by Wheeler, Seets, and Mullins[32,33] show that although a temperature induced lowering was observed the sticking probability at T_p around 1000 K remained still high enough for an efficient incorporation of the adsorbed oxygen for the exposures applied here. Thus, an expected decrease of the sticking probability with coverage would not account for the total lack of oxygen as observed in TDS for $T_p>1150$ K. The second alternative is more likely. For experimental confirmation we tried to detect the emission of RuO_3 molecules which exposing the Ru surface kept at $T_p=1300$ K to an intense oxygen beam. For the highest achieved molecular flux of 4×10^{14} cm^{-2} s^{-1}, no gas-phase RuO_x molecules could be detected, however, even when operating our mass spectrometer at the highest sensitivity. On the other hand, high-pressure oxidation experi-

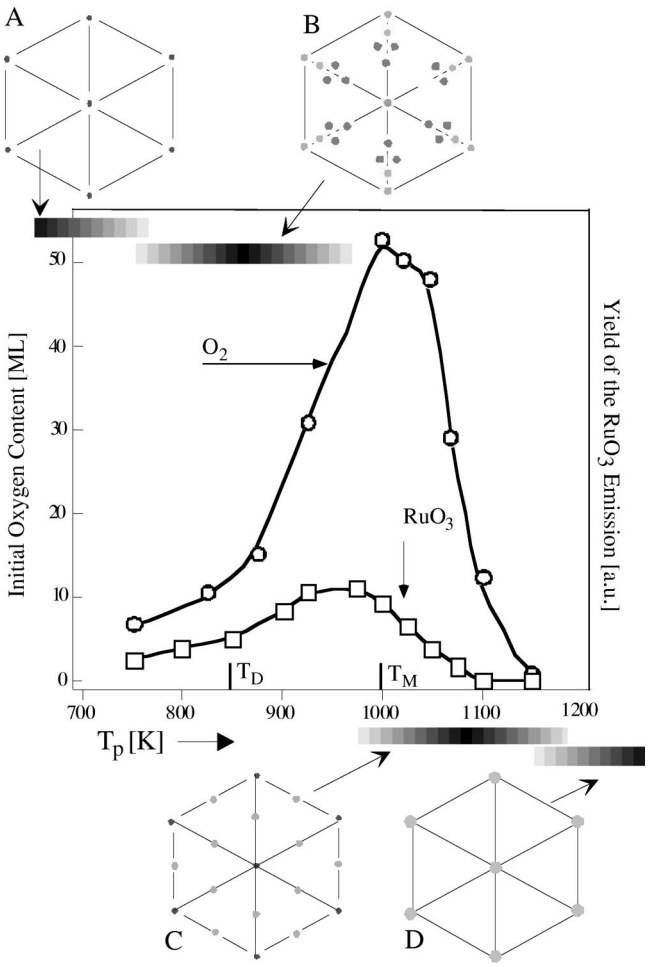

FIG. 5. Total oxygen content (open circles) and the RuO_3 emission (open squares) vs preparation temperature T_p. The curves result from the integration of the TD profiles presented in Fig. 4. The oxidation conditioned geometrical structure of the surface is represented here by four schemes of LEED patterns which are representative for the selected preparation regimes. All LEED images were taken at room temperature with an electron energy of 95 eV. The appearance regions for the characteristic LEED structures are shown as wrappers indicating roughly the relative intensity of the major spots.

ments with hot polycrystalline Ru wires show rather high partial pressures of RuO_3 and RuO_4 vapors even at temperatures lower than 1000 K.[34,35] However, these experimental conditions correspond to equilibrium between the Ru surface and the gas phase which cannot be realized with our experimental setup. It should be emphasized that for samples oxidized at $T_p > 1000$ K the mass spectrum of the molecular fragments emitted exhibits a new peak due to the emission of RuO_4 molecules, which has been completely absent for samples oxidized at $T_p < 1000$ K.

In order to support the presence of stable Ru oxides, the above-presented TD study was supplemented by a simple qualitative LEED analysis. The four LEED patterns shown in Fig. 5 (A, B upper part and C, D lower one) represent the main classes of LEED pattern observed in the whole temperature region between 300 and 1600 K. The gray horizontal bars indicate the mean spot intensity and the temperature regions where the corresponding patterns appear. Structure A has been described previously.[26,27,39] It represents a saturated layer of adsorbed oxygen atoms where the adatoms occupy the threefold coordinated hcp sites. The characteristic (1×1)-O spots are the only features for oxidation temperatures T_p up to about 700 K. The presence of this (1×1)-O structure also signifies the formation of a subsurface-oxygen phase without a significant admixture of RuO_x complexes.[7] For higher T_p ($T_D < T_p < T_M$) the brightness of the (1×1)-O spots substantially fades and a large number of additional weak spots starts to dominate the LEED images. Since a detailed structural analysis of such a complex pattern is beyond of the scope of this work, we selected only the most intense spots from the new pattern (pattern B) as simple markers for the formation of domains differing from the (1×1)-O adsorbed layer. For $T_p > T_M$, the corresponding LEED patterns reveal the formation of a well ordered phase of clear symmetry (pattern C). In addition to the very intense (1×1) reflexes, well ordered and sharp (2×2) spots appear suggesting the formation of a modified RuO_2 crystal phase. The (110) and the (100) surfaces of RuO_2 have been studied by the means of LEED, Auger, and x-ray photoelectron spectroscopy (XPS).[21] Both faces undergo a series of reversible reconstructions which result from preparation-dependent loss of surface oxygen. The corresponding pattern changed from (1×1) via $c(2\times2)$ into hexagonal or $p(1\times2)$. The agreement of the symmetry of pattern C with the hexagonal structure of the reconstructed RuO_2 crystal surfaces suggests that the corresponding surface is covered by a RuO_2 layer.

When performing the oxidation at $T_p > 1300$ K where, if any, only a tiny amount of oxygen remains at the topmost layer, pattern C undergoes a dramatic transformation. The LEED images (pattern D) nearly resemble the ones observed for an oxygen monolayer adsorbed on Ru(0001). The observed sequence of LEED patterns supports the notion of four temperature regions with respect to the state of the resulting oxygen phase: $T_p < T_D$ the oxygen phase created consists mainly of mobile oxygen atoms dissolved in the subsurface region. Partial transformation into oxides occurs for $T_D < T_p < T_m$. At $T_p > T_m$ the highly symmetric LEED pattern indicates the formation of an ordered oxide phase. Above 1200 K no oxides remain at the surface.

The identification of two quite distinct oxidation regimes ($T_p < T_D$ and $T_p > T_m$) calls for looking also at the electronic properties of the resulting oxygen phases. The electronic structure of oxidized surfaces has been usually analyzed by applying the XPS, e.g., Refs. 21 and 36. The binding energies of the Ru-3d and O-1s core states were taken as a simple electronic probe of the oxygen states created. Unfortunately, the oxidation of a ruthenium surface is merely reflected by a gradual broadening and an intensity increase of the respective peaks prohibiting a definite distinction between subsurface oxygen and the oxide formation.[14] Therefore, we focus here on the electronic modifications of the valence band induced by oxidation. Figure 6 shows two representative HeI-UP spectra taken after performing the oxidation at 700 K (upper spectrum) and at 1000 K (lower one). The most intense feature in the upper spectrum, the peak at 4.4 eV, is characteristic for the subsurface-oxygen phase.[37,38] It has been attributed to the occupied O-2p state. For surfaces consisting of oxides only, the intense O-2p peak dis-

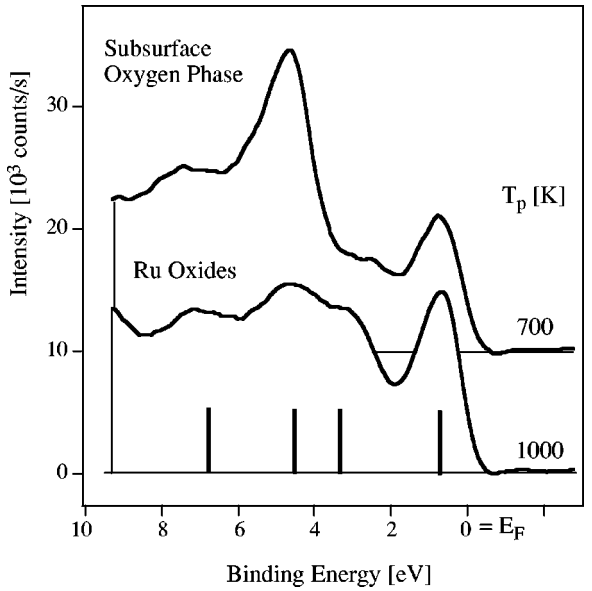

FIG. 6. Two UP(21.2 eV) spectra of the valence region taken after performing the oxidation at 700 K (upper spectrum) and at 1100 K (lower one). Under these preparation conditions the surfaces contained 5.1 and about 48 ML of oxygen, respectively. The upper spectra represents a surface containing only the mobile subsurface-oxygen phase whereas the lower one exhibits all symptoms of a solid RuO_2 phase. The vertical thin lines mark the energy positions of the major *d*-band features as predicted by the theory for RuO_2 phase.

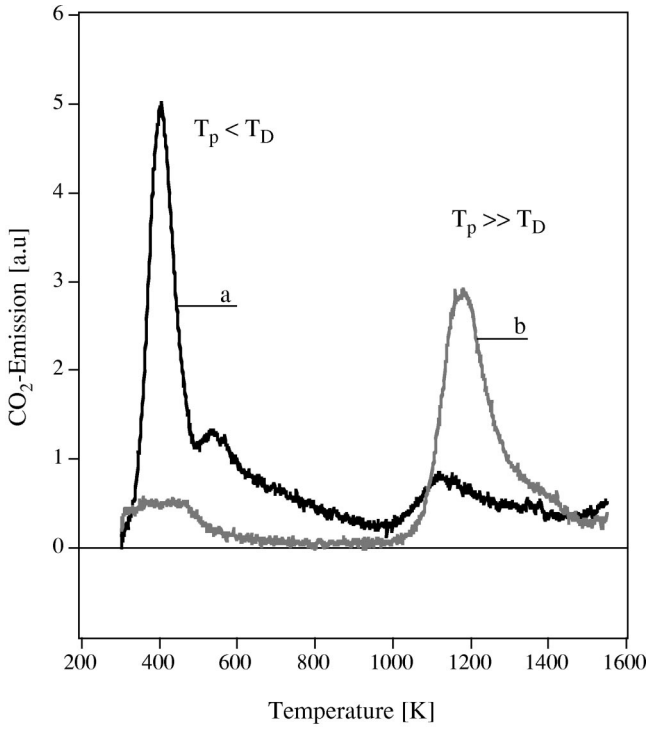

FIG. 7. CO_2 emission monitored from two different oxygen-rich Ru surfaces exposed to CO beam and heated with a constant rate up to 1600 K. The surfaces differed by the state of the major oxygen species deposited. The surface oxidized at 750 K contained about 7 ML of mobile oxygen atoms in the subsurface and the one oxidized at 1000 K was covered by an oxide film containing more than about 50 ML of oxygen. The CO flux carried by the beam was about 4×10^{14} cm^{-2} s^{-1}.

appears and is replaced by three weaker bands centered at 3.4, 4.6, and 7.2 eV. The peak at the Fermi level becomes more intense. These spectral features closely resemble the angle-integrated photoemission spectrum of a clean RuO_2 crystal published by Daniels *et al.*[38] The theoretical density of states for solid RuO_2 calculated by Mattheiss[40] is well reproduced by the main spectral features seen in our spectrum. The short vertical lines mark the energy positions of the centers of the theoretical peaks. They coincide quite well with our triplet structure. Thus, both the LEED and the UPS establish that the phase created by the oxidation of the ruthenium surface at $T_p > T_M$ represents a thick uniform RuO_2 film.

In the following we will amend the characterization of various oxygen species created at the surface by means of their reactivity. The CO/CO_2 conversion process is used here as a simple measure. Again, two representative samples were prepared by exposing the surface to the same oxygen dose at different sample temperatures (750 and 1000 K). As outlined previously, two distinct oxygen phases are created, the former containing about 7.1 ML of mobile subsurface oxygen, and the latter dominated by Ru oxides. As deduced from O_2 TD spectra, the oxide covered sample contains the large oxygen amount of about 49 ML. Subsequently, the prepared samples were exposed to a constant CO flux and heated with a constant rate (6 K/s) while the CO_2 flux was detected with a mass spectrometer. Figure 7 shows the CO_2 signal. The surface containing the subsurface-oxygen phase (curve a) exhibits a high reactivity in the low temperature region between 300 and 600 K which has been attributed to the high mobility of the dissolved oxygen atoms.[10] For the sample covered by the oxide layer (curve b) only a moderate conversion yield could be monitored at these temperatures. The yield starts to increase at the high temperature region between 1050 and 1100 K where, as shown previously, the decomposition of the RuO_2 layer takes place thereby supplying very efficiently the topmost surface layer with atomic oxygen. Unfortunately, as seen in Figs. 4(a) and 4(b), there exist at least two additional channels which reduce the residence time of the supplied oxygen atoms considerably: The oxygen desorption as well as the formation and emission of RuO_3. Both channels compete strongly with the CO oxidation and in consequence only a reduced conversion yield is observed. The dissociation limited reactivity of the RuO_2 layers contrasts with the diffusion limited reactivity of the subsurface oxygen phase, in particular in the activation energies of the process supplying the oxygen atoms for the CO oxidation reaction. As mentioned previously, for subsurface-oxygen the diffusion rate has been found to be very high due to the low activation energy of less than 0.3 eV.[10] In contrast for crystalline oxides this process is characterized by an almost ten times higher value of the activation barrier.[41]

Next, we will quantitatively check how the CO_2 yield depends upon the preparation temperature T_p. The integral CO/CO_2 conversion probability, γ, was determined by measuring the oxygen consumption upon exposure of the oxygen-rich surfaces to 10^3 L of CO (sample kept at 525 K). The surfaces investigated have been prepared by identical oxidation procedures at different temperatures T_p, covering a range from 500 to 1200 K. Figure 8 shows the function

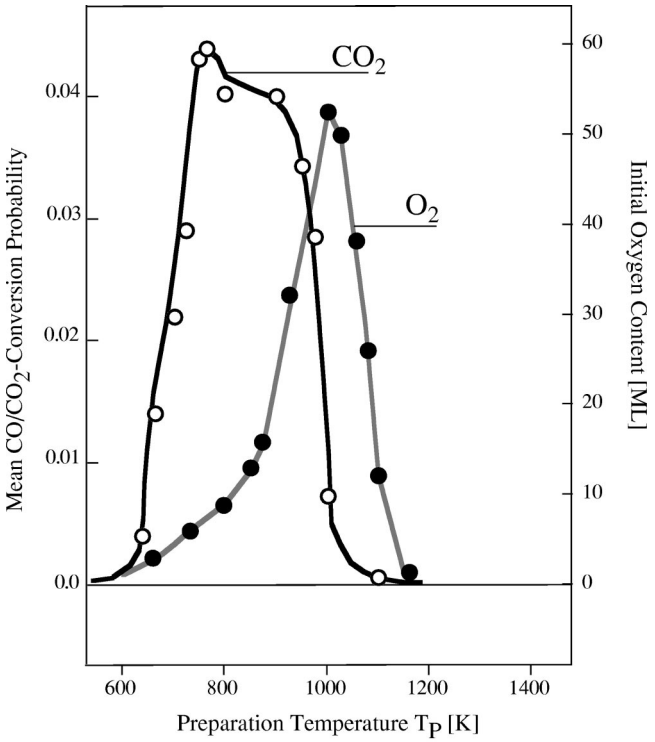

FIG. 8. The integral CO/CO_2 conversion probability vs oxidation temperature T_p (open circles). The results were obtained by measuring the oxygen consumption induced by exposing the oxygen-rich surfaces kept at 525 K to 10^3 L of CO. The reactivity is compared with the initial oxygen content deposited in the sample by exposing the surface to 5×10^5 L of oxygen (full circles).

$\gamma(T_p)$ (black line, open circles) together with the initial oxygen content, C_{init}, deposited at the sample, versus T_p (gray line, full circles). For $T_p<T_D$, where the sample contains predominantly subsurface oxygen, both functions increase with T_p. This concurrent behavior stops at $T_p>T_D$, where the further monotonic increase of C_{init} is associated with a drastic decrease of the conversion probability γ. For T_p around $T_M\approx1000$ K only a low reactivity was observed although a rather large oxygen content still remains in the surface (C_{init}, gray line). This reduction coincides with the temperature range where the formation of regular RuO_2 coating layers has been identified. For $T_p>T_M$ the mean reactivity drops to a value at least ten times smaller than the one obtained when subsurface oxygen is the dominating species. Thus, the presence of the oxide layers results in a significant reduction of the surface reactivity. Moreover, when the oxides become the dominating species and form a RuO_2 coating film, γ becomes extremely small comparable to the value known for CO oxidation performed at an oxygen submonolayer on a clean Ru(0001).[8] It must be emphasized that the conversion probability given is determined for the CO-oxidation reaction run at 525 K. At this temperature, the Ru oxides are stable and only the subsurface oxygen is active (see Fig. 7). The oxygen content on the other hand includes the total oxygen amount, i.e., also the nonreactive fraction captured in the oxide layers. However, the CO beam as applied here probes only the topmost layer of the surface. Thus it cannot be excluded definitely that the RuO_2 oxides form only a thin film blocking the access of subsurface oxygen to the surface. But such a configuration appears unlikely in view of the TD spectra in Fig. 4 and the UPS data in Fig. 6.

SUMMARY

The formation of various oxygen states appearing during the oxidation of a Ru(0001) surface has been characterized by the means of UPS, TDS, LEED and reactive scattering of a CO beam. For oxidation temperatures below the onset for oxygen desorption, T_D, the surface contains predominantly mobile and very reactive oxygen atoms in the subsurface region. Thermal removal of this oxygen is accompanied by the emission of various RuO_x ($x<4$) molecules which are formed dynamically from the subsurface oxygen at high temperatures. For preparation temperatures in between $T_D\approx850$ K and $T_M\approx1000$ K, both the content of dissolved oxygen and the RuO_x ($x<5$) emission increase with the preparation temperature T_p. The thermal removal of oxygen proceeds then via recombinative desorption as well as the decomposition of present oxides. The corresponding LEED patterns reveal a coexistence of oxidelike surface domains and regions terminated by the 1×1-O phase. Such a state, however, only slightly reduces the high initial reactivity of the surface. The situation changes dramatically when performing the oxygen exposure at even higher temperatures, $T_p>T_M$. The resulting new oxygen phase has been identified by LEED and UPS as a RuO_2 film which almost completely quenches the reactivity. All these experiments emphasize the unique properties of the subsurface-oxygen phase which in contrast to the oxide phase should be attractive to those real-world catalytic reactions where atomic oxygen is involved.

ACKNOWLEDGMENTS

Financial support by the DFG (Grant No. Ni-452) is gratefully acknowledged. A.B. is thankful for many elucidating discussions with G. Ertl and M. Scheffler from Fritz-Haber-Institute in Berlin.

[1] C. G. Bond, B. Coq, R. Dutartre, J. G. Ruize, A. D. Hooper, M. G. Proietti, M. C. S. Sierra, and J. C. Slaa, J. Catal. **161**, 480 (1996).
[2] F. Rosowski, A. Hornung, O. Hinrichsen, D. Herein, M. Muhlar, and G. Ertl, J. Appl. Crystallogr. **151**, 443 (1997).
[3] M. W. McQuire and C. H. Rochester, J. Catal. **157**, 396 (1995).
[4] D. L. Adams, L. E. Peterson, and C. S. Sorensen, J. Phys. C **18**, 1753 (1985).
[5] H. Samata, A. Mishiro, S. Sawada, Y. Nagata, T. Uchida, M. Kai, M. Ohtsuka, and M. D. Lan, J. Phys. Chem. Solids **59**, 1444 (1998).
[6] I. J. Malik and J. Hrbek, J. Phys. Chem. **95**, 10188 (1991).
[7] A. Böttcher and H. Niehus, J. Chem. Phys. **110**, 3186 (1999).
[8] A. Böttcher, H. Niehus, S. Schwegmann, H. Over, and G. Ertl, J. Phys. Chem. **101**, 11185 (1997).
[9] C. H. F. Peden and D. W. Goodman, J. Phys. Chem. **90**, 1360 (1986).
[10] A. Böttcher, M. Rogozia, H. Niehus, H. Over, and G. Ertl, J. Phys. Chem. **103**, 6267 (1999).
[11] K. A. Peterlinz and S. J. Sibener, J. Phys. Chem. **99**, 2817 (1995).
[12] J. Lauterbach, K. Asakura, and H. H. Rotermund, Surf. Sci. **313**, 52 (1994).
[13] H. H. Rotermund, J. Lauterbach, and G. Haas, Appl. Phys. A: Solids Surf. **57**, 507 (1993).
[14] J. Hrbek, D. G. van Campen, and I. J. Malik, J. Vac. Sci. Technol. A **13**, 1409 (1995).
[15] B. A. Banse and B. E. Koel, Surf. Sci. **232**, 275 (1990).

[16] W. J. Mitchell and W. H. Weinberg, J. Chem. Phys. **104**, 9127 (1996).
[17] I. J. Malik and J. Hrbek, J. Vac. Sci. Technol. A **10**, 2565 (1992).
[18] A. Böttcher and H. Niehus, Phys. Rev. B **60**, 143967 (1999).
[19] T. E. Madey, H. A. Engelhardt, and D. Menzel, Surf. Sci. **48**, 304 (1975).
[20] E. Hulpke, *Helium Atom Scattering from Surfaces* (Springer, Berlin, 1992).
[21] Lj. Atanasoska, W. E. O'Grady, R. T. Atanasoski, and F. H. Pollak, Surf. Sci. **202**, 142 (1988).
[22] G. K. L. Cranstoun, D. R. Pyke, and G. D. W. Smith, Appl. Surf. Sci. **2**, 375 (1979).
[23] G. K. L. Cranstoun and D. R. Pyke, Appl. Surf. Sci. **2**, 359 (1979).
[24] I. Surnev, G. Rangelov, and G. Bliznakov, Surf. Sci. **159**, 299 (1985).
[25] K. I. Kostov, M. Gsell, P. Jacob, T. Moritz, W. Widdra, and D. Menzel, Surf. Sci. **394**, L138 (1997).
[26] C. Stampfl, S. Schwegmann, H. Over, M. Scheffler, and G. Ertl, Phys. Rev. Lett. **77**, 3371 (1996).
[27] C. Stampfl and M. Scheffler, Phys. Rev. B **54**, 2868 (1996).
[28] J. Emsley, *The Elements* (Clarendon, Oxford, 1989), p. 164.
[29] J. A. Rard, Chem. Rev. **85**, 1 (1985).
[30] D. L. Cocke, G. Abend, J. H. Block, and N. Kruse, Langmuir **1**, 507 (1985).
[31] A. B. Anderson and M. K. Awad, Surf. Sci. **183**, 289 (1987).
[32] M. C. Wheeler, D. C. Seets, and C. B. Mullins, J. Chem. Phys. **105**, 1572 (1996).
[33] M. C. Wheeler, D. C. Seets, and C. B. Mullins, J. Vac. Sci. Technol. A **14**, 1572 (1996).
[34] H. Schäfer, A. Trebben, and W. Gerhard, Z. Anorg. Allg. Chem. **321**, 41 (1963).
[35] C. B. Alcock and G. W. Hooper, Proc. R. Soc. London, Ser. A **254**, 551 (1961).
[36] K. S. Kim and N. Winograd, J. Catal. **35**, 66 (1974).
[37] A. Böttcher and H. Niehus, Phys. Status Solidi A **173**, 101 (1999).
[38] R. R. Daniels, G. Margaritondo, C. A. Georg, and F. Levy, Phys. Rev. B **29**, 1813 (1984).
[39] P. He and K. Jacobi, Phys. Rev. B **55**, 4751 (1997).
[40] L. F. Mattheiss, Phys. Rev. A **13**, 2433 (1976).
[41] D. Shaw, *Atomic Diffusion in Semiconductors* (Plenum, London, 1973).